Article

Facile and Low-Cost Preparation of Nb/Al Oxide Catalyst with High Performance for the Conversion of Kiwifruit Waste Residue to Levulinic Acid

Rui Wang *, Xiaolin Xie, Yanxiu Liu, Zhigang Liu, Guofang Xie, Ning Ji, Lizhi Ma and Mingquan Tang

Guizhou Engineering Research Center for Fruit Processing, Food and Pharmaceutical Engineering Institute, Guiyang University, Guiyang 550003, China; E-Mails: xiaolinxie2015@126.com (X.X.); 15285973874@163.com (Y.L.); zhi_gang_liu@163.com (Z.L.); xieguofang616@sina.com (G.X.); jining552100@163.com (N.J.); malizhi2518@163.com (L.M.); tangmingquan2012@126.com (M.T.)

* Author to whom correspondence should be addressed; E-Mail: gzgpzx2012@sohu.com; Tel.: +86-851-8540-7613; Fax: +86-851-8540-7613.

Academic Editor: Rafael Luque

Abstract: The kiwifruit industry is booming worldwide. As a result, a great deal of kiwifruit waste residue (KWR) containing monosaccharides is produced and discarded. This material shows great potential for the production of platform chemicals. In this study, a series of Nb/Al oxide catalysts were synthesized via a facile and low-cost coprecipitation method, and their structures were characterized using: thermal gravimetric analysis (TGA), XRD, FESEM, TEM, X-ray photoelectron spectroscopy (XPS), NH_3-TPD, N_2 adsorption-desorption, and FTIR-Pyridine adsorption. Experimental results of sugar-to-levulinic acid (LA) conversion revealed that the 20% Nb/Al oxide catalyst provided the highest catalytic performance and durability in terms of LA yield from fructose (74.2%) at 463 K after 10 min and from glucose (47.5%) at 473 K after 15 min. Notably, the 20% Nb/Al oxide catalyst with a 10% dosage is capable of converting kiwifruit waste residue to LA at 473 K after 10 min. In conclusion, the enhanced catalytic performance was obtained due to the high acidity, and large surface area of Nb/Al oxide catalyst.

1. Introduction

Recently, the development of efficient approaches for the transformation of renewable sources into useful chemicals and fuels is an attractive research area because these technologies aim to conserve resources and create sustainable industrial practices [1]. As a promisingroute, conversion of the individual monomeric components like C6 or C5 sugars is currently available to make platform molecules with improved yields [2–4]. Amongst a range of potential bio-based chemicals, levulinic acid (LA) is considered a versatile building block for the production of valuable chemicals and biofuels, such as γ-valerolactone, pentanoic acid, and 2-methyltetrahydrofuran [5–7].

The use of feedstock is stilla principaltechnological barrier in the biomass industry. Currently, purified C6 mono- and disaccharides (e.g., fructose, glucose and sucrose) are frequently chosen as substrates. These sugars increase the production cost of industrial products and negatively impact the global food supply due to their use in both industries. However, the use of food supply chain waste (FSCW) as a renewable biorefinery is attractive, considering that massive food waste is generated and discarded in countries with high population densities [8]. The use of citrus peel, waste cooking oil and spent coffee grounds in countries such as China, the UK, Tanzania, Spain, Greece and Morocco has been studied, providing comprehensive and multidisciplinary approaches on the basis of advanced and innovative food valorization practices [9,10]. An example of this is seen in the production of LA fromsugar-rich acidic wastewater originating from the starch industry. A high yield of LA (91.41%) was produced by a sequential dehydration and rehydration process at 140 °C after 240 min [11].

Another challenge in biomass conversion is the use of heterogeneous acid catalysts with high performance. Taking into consideration the advantages of heterogeneous catalysis compared to heterogeneous acid catalysts, various solid acids, such as SO_3H-functionalized materials, zeolites, ionic-liquid-based hybrids, sulfated/phosphated metal oxides, and supported catalysts, have recently been developed for the sugar-to-LA conversion [12–17]. In a recent report, water was shown to be capable of dispersing sugars and was a better solvent for producing LA from C6 sugar monomer/oligomers, than organic solvents such as tetrahydrofuran and toluene [18]. However, the stability and selectivity of most solid acid catalysts, such as titania, zirconia, sulfated zirconia, and zirconium phosphate are found to be unsatisfactory in water, even at high reaction temperatures [19]. As a promising candidate, hydrated niobium pentoxide (or niobic acid, $Nb_2O_5 \cdot nH_2O$) is very acidic (pH ≥ −5.6, corresponding to 70% H_2SO_4) and exhibits high stability in acid catalyzed reactions when water molecules participate [20].

To further improve the structural properties as well as product selectivity, we have taken measures to optimize the conditions. For example, $Nb_2O_5 \cdot nH_2O$ treated with 1 M phosphoric acid and calcined at 300 °C was found to have larger surface area and stronger acidic properties. This can give a maximum 5-hydroxymethylfurfural selectivity of 100% in fructose dehydration [21]. Likewise, structure-directing agents such as L64, P103, P123, and porous solid supports (e.g., MCM-41 and

SBA-15) are also capable of enhancing the surface area of $Nb_2O_5 \cdot nH_2O$ and this increases the performance of xylose-to-furfural dehydration [22–24]. Despite the advantages, the acid waste that can be generated in the preparation of acid-treated $Nb_2O_5 \cdot nH_2O$ catalysts, and the use of templates to modify $Nb_2O_5 \cdot nH_2O$ is expensive.

Kiwifruit is widely cultivated in southern China, and the total production was over 1.17 million tons in 2014. About 37% of the fruit was processed into juice and chips, with residual peels accounting for 3–5 wt. % of the fruit. Notably, the levels of fructose and glucose are higher than that of sucrose in almost all the kiwifruit genotypes cultivated [25]. Thus there is great potential for the production of LA from the waste residue of the kiwifruit industry. Here, we present, a cost-effective, facile production method for LA from kiwifruit waste residue (KWR) that uses an Nb/Al mixed metal oxides prepared by coprecipitation with ammonium hydroxide. We found that the use of 20% Nb/Al oxide catalyst results in the highest yield of LA (~75%) from fructose at 463 K after 10 min. We also observed a moderate LA yield of ~50% from glucose at 473 K after 15 min. Moreover, the 20% Nb/Al oxide was capable of directly converting KWR to LA with a high catalytic performance at 463 K within 15 min.

## 2. Results and Discussion

2.1. Catalyst Characterization

From XRD patterns (Figure 1), we observed amorphous structure in all catalyst samples analyzed except Al_2O_3 and 10% Nb_2O_5/nano-Al_2O_3. In the case of Al_2O_3 and 10% Nb_2O_5/nano-Al_2O_3 samples, the broad peak at the range of 42°–48° was identified as γ-alumina [26]. In comparison to the XRD patterns of Al_2O_3 and Nb_2O_5, no obvious diffraction peak belonging to Nb_2O_5 was observed on the surface of 10% Nb_2O_5/nano-Al_2O_3, indicating that Nb_2O_5 was found within the pores of nano-Al_2O_3. When Nb and Al were hybridized via a coprecipitation method, a series of catalyst samples were prepared in the amorphous phase. Within this samples, the peak intensity located at 25° increased with the increase of Nb_2O_5 loading, This result, combined with the results from the analysis of N_2 adsorption-desorption isotherms (Figure 2), and FESEM, TEM (Figure 3), attributed this increase in peak intensity to an increase in the Nb species homogeneously dispersed in the mesoporous framework. To further investigate the surface composition of Nb/Al metal oxide catalyst samples, XPS measurement was performed, and surface composition of Nb/Al oxide catalysts was listed in Table 1.

The textural properties of Al_2O_3, 10% Nb_2O_5/nano-Al_2O_3, Nb_2O_5, and a series of Nb/Al oxide catalysts were analyzed using N_2 adsorption-desorption isotherms (Figure 2). Among these samples, Nb_2O_5 and 10% Nb_2O_5/nano-Al_2O_3 displayed type III isotherms with type H3 hysteresis loops. The Al_2O_3 and Nb/Al oxide catalysts presented in Figure 2 showed type IV isotherms with type H2 hysteresis loops, indicative of uniform mesoporous structure. FESEM and TEM images verified that the mesporous structure of Nb/Al oxide samples was generated by the aggregation and connection of nano-sized particles (Figure 3). When the Nb/Al ratio increased, the hysteresis loop gradually shifted to a higher relative pressure, probably owning to the formation of mesoporous structures introduced by Nb species. Correspondingly, the AD of mesoporous Nb/Al oxide samples increased from 3.97 nm to 5.45 nm as the samples with Nb dosage increased from 10% to 25% (Table 1). In contrast, SSA

gradually decreased within this range. It was interesting to notice that the SSA of Nb/Al oxide samples was larger than that of other samples (264.84 m^2/g–296.55 m^2/g *vs.* 108.06 m^2/g–207.77m^2/g).
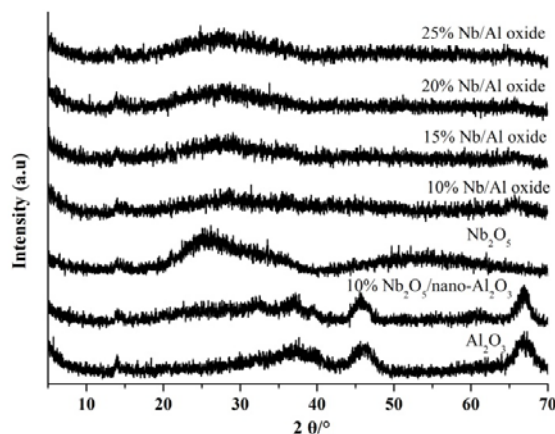
Figure 1. XRD patterns of Al₂O₃, 10% Nb₂O₅/nano-Al₂O₃, Nb₂O₅, and a series of Nb/Al oxide catalysts.
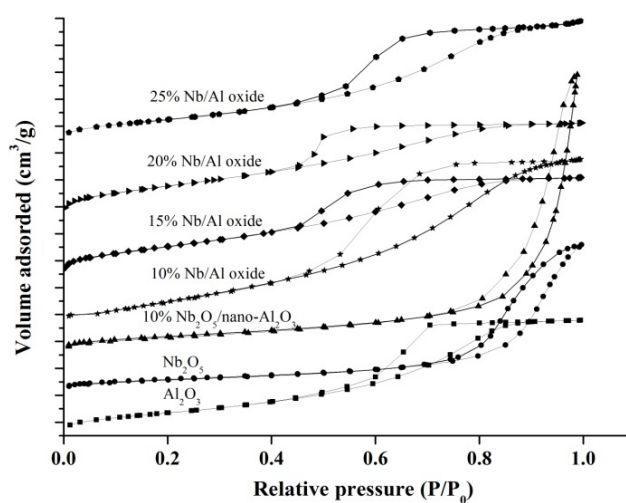
Figure 2. Nitrogen adsorption isotherms of Al₂O₃, 10% Nb₂O₅/nano-Al₂O₃, Nb₂O₅, and a series of Nb/Al oxide catalysts.
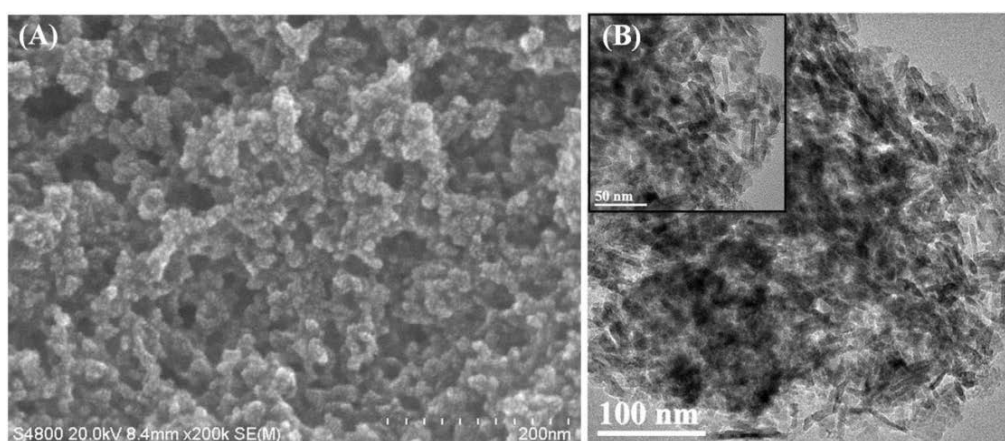
Figure 3. FESEM (**A**); and TEM (**B**) images of 20% Nb/Al oxide.

Table 1. Textural properties, surface composition, and NH₃-TPD characterization of the catalyst samples.

Catalysts	SSA (m^2/g)	AD(nm)	Surface Composition	Weak Acidity (%) 373–573 K	Moderate Acidity (%) 573–773 K	Strong Acidity (%) >773 K	Total Acidity (mmol/g)
10% Nb/Al oxide	296.55	3.97	$Nb_{0.036}Al_{2.437}O_{2.713}$	34.6	65.4	0	2.11
15% Nb/Al oxide	288.98	4.20	$Nb_{0.045}Al_{1.706}O_{2.472}$	41.0	0	59.0	1.66
20% Nb/Al oxide	281.47	4.49	$Nb_{0.077}Al_{1.001}O_{1.761}$	38.1	0	61.9	1.81
25% Nb/Al oxide	264.84	5.45	$Nb_{0.081}Al_{0.989}O_{1.059}$	39.8	0	60.2	1.79
10% Nb_2O_5/nano-Al_2O_3	142.34	22.83	-	75	0	25	0.40
Nb_2O_5	108.06	16.02	-	58.5	8.9	32.6	0.77
Al_2O_3	207.77	5.69	-	98.8	0	1.2	0.83

NH₃-TPD was employed to study the acid strength and contents of catalyst samples based on desorption temperatures and integral areas of specific peaks, respectively. As shown in Figure S1, all samples exhibited a high NH₃ desorption peak centered at ~323 K, which is representative of weak acid sites. Surprisingly, additional peaks were detected around 823 K, confirming the presence of strong acid sites, and these increased with the increasing Nb content. Additionally, the acid concentrations were calculated according to the amount of adsorbed NH₃, as listed in Table 1. 10% Nb_2O_5/nano-Al_2O_3 was showed a slightly lower acid content (0.40 mmol/g) than Al_2O_3 and Nb_2O_5 (0.77 and 0.83 mmol/g, respectively). In the case of the Nb/Al oxide catalysts, the total acid content decreased by increasing the Nb/Al ratio, but the concentration of strong acid sites increased. Among them, 20% Nb/Al oxide had the highest proportion of strong acid sites and total acidity (61.9% and 1.81 mmol/g, Table 1). Combined with the surface composition of Nb/Al oxide catalysts listed in the Table 1, it was deduced that Nb/Al oxide catalysts with the proper Nb/Al ratios would not only offer a mesoporous structure, but also enhance the acidic strength. There was no obvious difference in the AD of Nb/Al oxide catalysts (3.97 nm–5.45 nm, Table 1). Furthermore, the Brønsted and Lewis acid sites on the surface of catalyst samples were distinguish by FTIR-Pyridine adsorption, and concentrations of two different acid sites were quantified by a previous report [27]. As shown in Figure S2 and Table S1, when Nb/Al oxide catalysts were prepared by coprecipitation method, the concentration of Brønsted and Lewis acid sites were increased obviously compared to solo Al_2O_3 and Nb_2O_5. With the increase of Nb species on the surface, the rations of Brønsted to Lewis were also raised. This is because Bronsted acid sties are mainly responsible for the decomposition or hydrolysis of glucose to fructose [27]. We speculated that 20% Nb/Al oxide with high SSA (281.47 m^2/g), high strong acidity (61.9%), total acidity (1.73 mmol/g) and ration of Brønsted to Lewis would provide the most active sites for the catalytic system.

2.2. Catalytic Reaction

2.2.1. Catalytic Conversion of Glucose and Fructose to LA with Different Metal Oxide Catalysts

Considering that KWR is mainly composed of fructose and glucose [25], initial experiments were carried out using different metal oxide catalysts to convert glucose and fructose into LA (Figure S3).

As shown in Figure S3A$_1$, a moderate glucose conversion of 59.6% with 26.6% selectivity to LA was obtained using 10%Nb/Al oxide as the catalyst prepared by coprecipitation method. This method was much more active than 10%Nb$_2$O$_5$/nano-Al$_2$O$_3$ prepared by impregnation in a short reaction time of 10 min at 453 K. Although Al$_2$O$_3$ and Nb$_2$O$_5$ exhibited much higher glucose conversion than 10%Nb$_2$O$_5$/nano-Al$_2$O$_3$, the selectivity and the yield of LA was lower. In the case of the conversion of fructose to LA (Figure S3A$_2$), comparable fructose conversions were observed among the catalyst samples examined under identical reaction conditions as used for glucose. All of the fructose conversions analyzed demonstrated significantly higher conversion rates than the corresponding rates of glucose transformation. Notably, the10% Nb/Al oxide catalyst exhibited the highest selectivity for LA conversion, thus affording a relatively higher LA yield from fructose. These results were consistent with the acidity and texture of the catalyst samples (Table 1). Therefore, 10% Nb/Al oxide could convert both glucose and fructose into LA, and therefore was chosen for our subsequent studies.

2.2.2. Effect of Nb Loading of Nb/Al Oxides on Catalytic Conversion of Glucose and Fructose to LA

In comparison with solo Al$_2$O$_3$, the addition of Nb to form 10% Nb/Al oxide increased the selectivity of LA, as illustrated in Figure S3A$_1$,A$_2$. To evaluate the influence of Nb loading, further experiments on the catalytic conversion of glucose and fructose to LA over Nb/Al oxides with different Nb loadings were undertaken at 453 K after 10 min (Figure S3B$_1$,B$_2$. Substance conversion and LA selectivity/yield simultaneously increased with the increase of Nb loading from 10% to 20% in both glucose and fructose conversions. LA selectivity and yield started to decrease as the Nb loading increased to 25% in the process of fructose conversion. The relatively high acid strength and content appeared to assist the sugar conversion, while excess acid sites seemed to cause side reactions. With respect to glucose transformation, LA selectivity and yield did not attenuate until Nb loading was above 20%. From an economic point of view, 20% Nb/Al oxide was a superior catalyst for both glucose and fructoseLA conversion.

2.2.3. Effect of Reaction Temperature on Catalytic Conversion of Glucose and Fructose to LA with 20% Nb/Al Oxide

Reaction temperature is generally considered an important parameter in determining the yield of product. The effect of temperatures from 453 to 483 K on the catalytic activity of 20%Nb/Al oxide was studied, while other experimental conditions were kept constant. The results shown in Figure S3C$_1$,C$_2$ revealed that LA selectivity and yield increased with an increase in temperature, reaching around 49.1% and 41.3% for glucose at 473 K, and 69.2% and 70.2% for fructose at 463 K. When the reaction temperature was continuously increased until it reached 483 K, glucose conversion reached nearly 100%, but LA yields dropped to 21.1%. This was because of substrate and product decomposition at such high temperatures. Humin, one of the side products, was found in the reaction mixtures obtained under high temperature, a result, which was also observed previously [28]. Therefore, the optimum reaction temperatures of 473 K for glucose and 463K for fructose were employed in the subsequent experiments.

2.2.4. Effect of 20% Nb/Al Oxide Dosage on the Catalytic Conversion of Glucose and Fructose to LA

The effect of different catalyst dosages of 20% Nb/Al oxide on the production of LA from glucose and fructose was investigated after a reaction time of 10 min at 473 K and 463 K, respectively (Figure S3D$_1$,D$_2$). The addition of 20% Nb/Al oxide was found to be efficient in the conversion of both glucose and fructose to LA. When the catalyst dosage was increased from 5 to 10 wt. %, the LA yields increased slightly and were found to be 43.5% and 74.2% for glucose and fructose, respectively. Catalytic sites increased with the increasing catalyst dosage, and this was proposed to boost the sequential dehydration-rehydration reaction. However, further increasing the dosage of 20% Nb/Al oxide sharply decreased LA yields, although a slight increase of LA yield and selectivity were detected with a catalyst dosage of 15 wt. %. It appears that the high catalyst dosage not only accelerated the conversion of fructose into LA, but also promoted other side reactions such as cross-polymerization reactions and humin formation. These results showed that the catalyst dosage of 10 wt. % was appropriate for the conversion of glucose and fructose into LA in this catalytic system.

2.2.5. Effect of Reaction Time on Catalytic Conversion of Glucose and Fructose to LA with 20% Nb/Al Oxide

As discussed above, the conversion rates and product selectivity for glucose and fructose were greatly affected by the number of active sites. Likewise, the contact time between substrate and active sites was also investigated. For glucose conversion, the substrate conversion rate as well as LA selectivity and yield gradually increased when the time increased from 5 to 15 min, with a maximum LA yield of 47.5%. In contrast, the conversion of fructose to LA was not as sensitive to the reaction time, and a slight increase in LA yield and selectivity was observed with the exception of a sudden increase in conversion from 5 to 10 min. When we further increased the time to 15 and 20 min, fructose conversion kept almost constant while the selectivity and yield of LA were uniformly decreased. Combined with our previous results, the optimal reaction conditions for glucose (10 wt. % of 20% Nb/Al oxide, 473 K, 15 min) and fructose (10 wt. % of 20% Nb/Al oxide, 463 K, 10 min) were clarified.

2.2.6. Catalytic Transformation of KWR into LA

Initially, the average glucose and fructose content in the filtrate of treated KWR was determined by HPLC, and were found to be 6.7 mg/mL and 14.5 mg/mL, respectively. Since kiwifruit mainly consist of glucose, fructose and a small amount of sucrose [25], the optimized reaction conditions clarified in above sections for converting both glucose and fructose to LA were thus adopted. LA concentration (mg/mL) was used as anindex. Formic acidis one of the main by-products when producing LA from a hexose sugar [29]. Therefore, four conditions wereadopted and screened in the present study. As shown in Table 2, 94.3% of fructose and moderate conversion of glucose (62.6%) were detected in the presence of 10 wt. % of 20% Nb/Al oxide at 463 K within 10 min, giving an LA concentration of 9.2 mg/mL (Entry 1). No significant increase in sugar conversion, as well as LA concentration, was achieved when the reaction time increased from 10 to 15 min (Table 2, Entry 2), especially for glucose. It appeared that fructose was easier to convert to LA, compared with glucose [29,30]. On the

other hand, the shift of isomerization equilibrium from glucose to fructose was suppressed by the high fructose/glucose ratio of 2.18, thus leading to more glucose remaining in the reaction mixture. As the optimal reaction conditions for the conversion of glucose to LA were employed, a slight increase in sugar conversion was observed (Table 2, Entry 4). LA concentration (8.5 mg/mL) was lower than that carried out under other reaction conditions (9.2–9.8 mg/mL), indicating the occurrence of side reactions, particularly, in the case of fructose degradation (Table 2). Shortening the reaction time from 15 min to 10 min, the LA concentration increased from 8.5 to 9.0 mg/mL with almost unchanged sugar conversion. This could likely be attributed to lower downstream conversion of LA through reactions like condensation and polymerization. From our prior discussion, it can been seen that the transformation of KWR in the presence of 10 wt. % of 20%Nb/Al oxide at 463 K for 15 min showed an enhanced LA concentration. To study the reusability of 20%Nb/Al oxide in the process of KWR-to-LA conversion, five consecutive reaction cycles were carried out by simple treatment of the catalyst with a deionized watewash and calcination at 800 K for 1 hafter the end of each run. Under the optimized reaction conditions of KWR-to-LA transformation, the LA concentration obtained through five sequential runs was 9.8 mg/mL, 9.2 mg/mL, 9.8 mg/mL, 9.5 mg/mL, and 9.7 mg/mL, respectively. Furthermore, the leaching of Al and Nb elements in the KWR reaction mixture derived from 20% Nb/Al oxide catalyst was found to be 7.0 mg/L and 11.2 mg/L, respectively. Therefore, the almost constant catalytic performance in terms of increasing LA concentration illustrated the strong stability of the 20% Nb/Al oxide catalyst.

Table 2. Effect of reaction conditions on the catalytic conversion of kiwifruit waste residue (KWR) by 20% Nb/Al oxide.

Reaction Condition	Glucose Conversion (%)	Fructose Conversion (%)	LA Concentration (mg/mL)
10 wt. % of 20% Nb/Al oxide, 463 K, 10 min	62.6	94.3	9.2
10 wt. % of 20% Nb/Al oxide, 463 K, 15 min	67.3	97.3	9.8
10 wt. % of 20% Nb/Al oxide, 473 K, 10 min	71.2	98.8	9.0
10 wt. % of 20% Nb/Al oxide, 473 K, 15 min	76.2	99.3	8.5

3. Experimental Section

3.1. Materials

Glucose, fructose, Nano-Al_2O_3 (special surface area: 260 m^2/g), $NbCl_5$, and $Al(NO_3)_3 \cdot 9H_2O$ in analytical reagent-grade were purchased from Aladdin Chemistry Co., Ltd, Shanghai, China. All standards including glucose, fructose, and levulinic acid were purchased from Sigma-Aldrich, Saint Louis, MO, USA. The KWR sample was collected from Guizhou Engineering Research Center for Fruit Processing, China.

3.2. Glucose and Fructose Extraction from KWR

According to a previous report [1], the glucose and fructose content of KWR was determined as 16.41 mg/g and 34.39 mg/g, respectively. The extraction process was carried out in a round-bottom flask containing 100 g KWR with 200 mL distilled water, equipped with a stirrer. The mixture was heated at 333 K for 20 min, followed by filtration upon completion. The glucose and fructose content in the filtrate was determined by HPLC, which was found to be 6.7 mg/mL and 14.5 mg/mL, respectively.

3.3. Catalyst Preparation

Catalyst samples with different Nb to Al weight ratios of 10, 15, 20, and 25 wt. % were successively denoted as 10% Nb/Al, 15% Nb/Al, 20% Nb/Al, and 25% Nb/Al catalysts in this study. These samples were prepared using a facile and cost-effective aqueous ammonia coprecipitation method. In a typical procedure for the synthesis of 20% Nb/Al oxide, 0.1382 g of $NbCl_5$ and 5.0 g of $Al(NO_3)_3 \cdot 9H_2O$ were dissolved in 143.5 mL of anhydrous ethanol. This resulted in the formation of a total metal ion concentration of 0.1 mol/L. Under vigorous stirring, 2.5 mol/L aqueous ammonia solution was added dropwise into the above solution at the rate of one drop per second until the solution reached pH 7. The resulting sol was aged at 298 K for 24 h. Then, the ethanol in the aged sample was removed at 353K by rotary evaporation, followed by drying at 373K in the oven for 10 h. Based on the results from TGA (Figure S4), the catalyst precursor was calcined from room temperature to 800 K, for 1 h in static air. The entire process was performed using a heating rate of 4 $K \cdot min^{-1}$ under 50 $L \cdot h^{-1}$ airflow. For comparison, Nb_2O_5 and Al_2O_3 catalyst samples were prepared by the same procedure, while calcined at 700 K and 900 K (Figure S4), respectively.

10% Nb_2O_5/nano-Al_2O_3 catalyst was prepared by wetness impregnation. In detail, 0.4066 g $NbCl_5$ and 1 g nano-Al_2O_3 were mixed in 100 mL anhydrous ethanol and stirred at room temperature for 24 h. The mixture was then dried overnight in an oven at 373 K. Finally, the precursor was calcined according to the procedure of 20% Nb/Al oxide except the final temperature was 600 K (Figure S4).

3.4. Catalyst Characterization

The thermal gravimetric analysis (TGA) measurements were carried out using a Netzsch STA449C Jupiter TGA/DSC (NETZSCH, Selb, Germany) at a heating rate of 10 K/min under pure nitrogen, and approximately 10 mg sample was used. Powder XRD analysis was performed on a Bruker D8 Advanced X-ray diffractometer (Bruker, Karlsruhe, Germany) with Cu Kα radiation (λ = 0.154 nm) at 40 kV and 30 mA with a step size of 0.02. After determination, the background was deducted. The surface composition of the samples was analyzed by X-ray photoelectron spectroscopy (XPS) (Shimadzu, Tokyo, Japan) using Kratos Axis Ultra DLD system and a monochromatic Al Ka source operated at 15 keV and 150W. The detection area was 1200 μm × 800 μm. The binding energy value of each element was corrected using C1s signal as a reference at 284.6 eV. The morphologies of the catalyst sample were obtained by FESEM on a Hitachi S4800 (Hitachi, Tokyo, Japan). In addition, the microscopic features were obtained by TEM on a FEI Tecnai G2 F20 S-TWIN (FEI, Hillsboro, OR, USA) at 200 kV. First 3% of each sample powderwere dispersed in anhydrous ethanol by ultrasonication. Then, a porous carbon copper gridwas dipped into the suspension. Before analysis, the

grid was dried under a vacuum at 80 °C for 8 h. NH_3-TPD was conducted on an AutoChem 2920 chemisorption analyzer (Micromeritics, GA, American). Before adsorption, 50mg of the sample was loaded in a quartz U-tube reactorand pre-treated at 473K in helium for 1 h followed by cooling to 323 K. Then the catalyst samplewasintroduced at a flow of NH_3/Ar(10 *v/v*%) and then maintained for 1 h. Physiabsorbing NH_3 molecules were removed by flowing pure heliumat 323 K for 1 h. Finally, the temperature was raised to 1073 K at a rate of 10 K/min. Desorbed ammonia was detected with a thermal conductivity detector (TCD) (Micromeritics, GA, American).The specific surface areas (SSA) of the samples were recorded on a Micromeritics ASAP 2020 (Micromeritics, GA, American) at the liquid nitrogen temperature. Every sample was degassed for 3 h at 573 K, and then SSA was subsequently determined by the BETmethod over the relative pressure range $P/P_0 = 0.05$ to 0.20. Average pore diameter (AD) was deduced from desorption data by the Barrett-Joyner-Halenda (BJH) method. To investigate the Brønsted and Lewis acid sites of the catalyst samples, FTIR-Pyridine adsorption was performed by a Frontier FT-IR (PerkinElmer, Waltham, CT, USA). Every sample was degassed in the IR cell overnight at 673 K. The adsorption of Pyridine was performed at 250 °C for 1 h. The spectra were recorded at room temperature with a resolution of 4 cm^{-1}.The metal components of the catalyst leached into the reaction mixture were determined using inductively coupled plasma/optical emission spectrometry (700-ES, Varian, Salt Lake City, UT, USA). The KWR sample was pre-treated by microwave digestion. By weighing approximately 2 g of reaction mixture, 10 mL of concentrated HNO_3 (65%), and 3 mL of H_2O_2 (30%), the mixture was transported into vessel, then was closed and heated at 483 K for 10 min.

3.5. Catalyst Activity

The batch catalytic assay was performed in a 50 mL stainless steel vessel. Typically, 2 g substrate (e.g., glucose or fructose) was dissolved in 30 mL deionized water in the presence of a prescribed dosage of catalyst at a designated temperature and this was allowed to react for a specific reaction time. After the reaction was complete, the system was immediately immersed into an ice-salt bath to stop the reaction. Then, the reaction mixture was filtered and the residue was washed with deionized water 3 times. All experiments were carried out in triplicate. To investigate the reusability of the Nb/Al oxide catalyst, the reclaimed sample was collected and washed 3 times with deionized water and calcined in 800 K for 1 h in static air for the next run.

3.6. Product Analysis

All samples were filtered through a 0.45 μm membrane syringe filter before HPLC analysis and started using a previously reported method [1]. The concentrations of glucose and fructose were obtained by a HPLC (LC-15C, Shimadzu, Suzhou, China) equipped with a C_{18} column (4.6 × 250 mm, 5 μm) at 303K and a refractive index detector (RID-10A, Shimadzu, Tokyo, Japan). The mobile phase was set as ultrapure water/acetonitrile (3:7, *v/v*) at a flow rate of 1.0 mL/min. LA was quantified by UV detector (254 nm, SPD-15C, Shimadzu, Suzhou, China) with a mobile phase of methanol/0.1% formic acid solution (12:88, *v/v*) at a flow rate of 0.5 mL/min. The column temperature was kept at 303 K. Each sample was diluted with ultra pure water before analysis.Substrate (*i.e.*, glucose or fructose) conversion, LA yield, and product selectivity were defined as follows:

$$\text{Substrate conversion }(\%) = \frac{\text{initial substrate amount (g)-final substrate amount (g)}}{\text{initial substrate amount (g)}} \times 100\%$$

$$\text{LA yield }(\%) = \frac{\text{actual output (g)}}{\text{theoretical output(g)}} \times 100\%$$

$$\text{Product selectivity}(\%) = \frac{\text{LA yield(\%)}}{\text{substrate conversion }(\%)} \times 100\%$$

4. Conclusions

Among a series of Nb/Al oxides synthesized via a facile and cost-effective coprecipitation method, the 20% Nb/Al oxide catalyst exhibited superior performance in sugar-to-LA conversion. High LA yields of 74.17% and 47.52% could be obtained from fructose and glucose at 463 and 473 K after a reaction time of 10 and 15 min, respectively. The robust water-tolerance, high special surface area, acidity, and Brønsted acid concerntration of the Nb/Al oxide catalyst were considered to be responsible for the enhanced activity. Moreover, the 20% Nb/Al oxide was also able to convert KWR to LA, resulting in an excellent fructose conversion and a moderate glucose conversion. Importantly, no significant loss of activity was detected after the catalyst was recycled five times.

Acknowledgments

Author Contributions

The experimental work was conceived and designed by R.W., X.X. and L.M.; Y.L., G.X., and M.T. performed the experiments; R.W. and Z.L. analyzed the data; Z.L. and N.J. contributed reagents/materials/analysis tools; R.W. and X.X. drafted the paper. The manuscript was amended through the comments of all authors. All authors have given approval for the final version of the manuscript.

Conflicts of Interest

The authors declare no conflict of interest.

References

1. Bevilaqua, D.B.; Rambo, M.K.D.; Rizzetti, T.M.; Cardoso, A.L.; Martins, A.F. Cleaner production: Levulinic acid from rice husks. *J. Clean Prod.* **2013**, *47*, 96–101.
2. Uçkun Kıran, E.; Trzcinski, A.P.; Liu, Y. Platform chemical production from food wastes using a biorefinery concept. *J. Chem. Technol. Biotechnol.* **2015**, *90*, 1364–1379.

3. Jager, G.; Buchs, J. Biocatalytic conversion of lignocellulose to platform chemicals. *Biotechnol. J.* **2012**, *7*, 1122–1136.

4. Hu, X.; Wu, L.P.; Wang, Y.; Song, Y.; Mourant, D.; Gunawan, R.; Gholizadeh, M.;Li, C.Z. Acid-catalyzed conversion of mono- and poly-sugars into platform chemicals: Effects of molecular structure of sugar substrate. *Bioresour. Technol.* **2013**, *133*, 469–474.

5. Yan, K.; Lafleura, T.; Wu, G.S.; Liao, J.Y.; Ceng, C.; Xie, X.M. Highly selective production of value-added γ-valerolactone frombiomass-derived levulinic acid using the robust Pd nanoparticles. *Appl. Catal. A* **2013**, *468*, 52–58.

6. Yan, K.; Chen, A.C. Selective hydrogenation of furfural and levulinic acid to biofuelson the ecofriendly Cu-Fe catalyst. *Fuel* **2014**, *115*, 101–108.

7. Yan, K.; Lafleur, T.; Liao, J. Facile synthesis of palladium nanoparticles supportedon multi-walled carbon nanotube for efficient hydrogenationof biomass-derived levulinic acid. *J. Nanopart. Res.* **2013**, *15*, 1906–1913.

8. Pfaltzgraff, L.A.; de bruyn, M.; Cooper, E.C.; Budarin, V.; Clark, J.H. Food waste biomass: A resource for high-value chemicals. *Green Chem.* **2013**, *15*, 307–314.

9. Lin, C.S.K.; Pfaltzgraff, L.A.; Herrero-Davila, L.; Mubofu, E.B.; Abderrahim, S.; Clark, J.H.; Koutinas, A.A.; Kopsahelis, N.; Stamatelatou, K.; Dickson, F. Food waste as a valuable resource for the production of chemicals, materials and fuels. Current situation and global perspective. *Energy Environ. Sci.* **2013**, *6*, 426–464.

10. Liu, Y.; Sotelo-Boyás, R.; Murata, K.; Minowa, T.; Sakanishi, K. Production of Bio-Hydrogenated Diesel by Hydrotreatment of High-Acid-Value Waste Cooking Oil over Ruthenium Catalyst Supported on Al-Polyoxocation-Pillared Montmorillonite. *Catalysts* **2012**, *2*, 171–190.

11. Kraithong, W.; Viriya-empikul, N.; Laosiripojana, N. Catalytic Conversion of Wastewater from Starch Industry to Levulinic Acid. *Innov. Sys. Des. Eng.* **2014**, *5*, 1–5.

12. Li, K.; Bai, L.; Amaniampong, P.N.; Jia, X.; Lee, J.M.; Yang, Y. One-Pot Transformation of Cellobiose to Formic Acid and Levulinic Acid over Ionic-Liquid-based Polyoxometalate Hybrids. *ChemSusChem* **2014**, *7*, 2670–2677.

13. Morales, G.; Osatiashtiani, A.; Hernández, B.; Iglesias, J.; Melero, J.A.; Paniagua, M.; Brown, D.R.; Granollers, M.; Lee, A.F.; Wilson, K. Conformal sulfated zirconia monolayer catalysts for the one-pot synthesis of ethyl levulinate from glucose. *Chem. Commun.* **2014**, *50*, 11742–11745.

14. Ramli, N.A.S.; Amin, N.A.S. Catalytic hydrolysis of cellulose and oil palm biomass in ionic liquid to reducing sugar for levulinic acid production. *Fuel Process. Technol.* **2014**, *128*, 490–498.

15. Saravanamurugan, S.; Riisager, A. Zeolite catalyzed transformation of carbohydrates to alkyl levulinates. *ChemCatChem* **2013**, *5*, 1754–1757.

16. Upare, P.P.; Yoon, J.W.; Kim, M.Y.; Kang, H.Y.; Hwang, D.W.; Hwang, Y.K.; Kung, H.H.; Chang, J.S. Chemical conversion of biomass-derived hexose sugars to levulinic acid over sulfonic acid-functionalized graphene oxide catalysts. *Green Chem.* **2013**, *15*, 2935–2943.

17. Ramli, N.A.S.; Amin, N.A.S. Fe/HY zeolite as an effective catalyst for levulinic acid production from glucose: Characterization and catalytic performance. *Appl. Catal. B* **2015**, *163*, 487–498.

18. Hu, X.; Wang, S.; Westerhof, R.J.; Wu, L.; Song, Y.; Dong, D.; Li, C.Z. Acid-catalyzed conversion of C6 sugar monomer/oligomers to levulinic acid in water, tetrahydrofuran and toluene: Importance of the solvent polarity. *Fuel* **2015**, *141*, 56–63.

19. Yang, F.; Liu, Q.; Bai, X.; Du, Y. Conversion of biomass into 5-hydroxymethylfurfural using solid acid catalyst. *Bioresour. Technol.* **2011**, *3*, 3424–3429.

20. Tanabe, K.; Okazaki, S. Various reactions catalyzed by niobium compounds and materials. *Appl. Catal. A* **1995**, *133*, 191–218.

21. Armaroli, T.; Busca, G.; Carlini, C.; Giuttari, M.; Raspolli Galletti, A.M.; Sbrana, G. Acid sites characterization of niobium phosphate catalysts and their activity in fructose dehydration to 5-hydroxymethyl-2-furaldehyde. *J. Mol. Catal. A* **2000**, *151*, 233–243.

22. Nakajima, K.; Fukui, T.; Kato, H.; Kitano, M.; Kondo, J.N.; Hayashi, S.; Hara, M. Structure and Acid Catalysis of Mesoporous $Nb_2O_5 \cdot nH_2O$. *Chem. Mater.* **2010**, *22*, 3332–3339.

23. García-Sancho, C.; Rubio-Caballero, J.M.; Mérida-Robles, J.M.; Moreno-Tost, R.; Santamaría-González, J.; Maireles-Torres, P. Mesoporous Nb_2O_5 as solid acid catalyst for dehydration of dxylose into furfural. *Catal. Today* **2014**, *234*, 119–124.

24. García-Sancho, C.; Agirrezabal-Telleria, I.; Güemez, M.B.; Maireles-Torres, P. Dehydration of dxylose to furfural using different supported niobia catalysts. *Appl. Catal. B* **2014**, *152–153*, 1–10.

25. Esti, M.; Messia, M.C.; Bertocchi, P.; Sinesio, F.; Moneta, E.; Nicotra, A.; Fantechi, P.; Palleschi G.Chemical compounds and sensory assessment of kiwifruit (*Actinidia chinensis* (Planch.) var. *chinensis*): Electrochemical and multivariate analyses. *Food Chem.* **1998**, *61*, 293–300.

26. Zhu, H.Y.; Riches, J.D.; Barry, J.C. γ-Alumina Nanofibers Prepared from Aluminum Hydrate with Poly(ethylene oxide) Surfactant. *Chem. Mater.* **2002**, *14*, 2086–2093.

27. Emeis, C.A. Determination of Integrated Molar Extinction Coefficients for Infrared Absorption Bands of Pyridine Adsorbed on Solid Acid Catalysts. *J. Catal.* **1993**, *141*, 347–354.

28. Ya'aini, N.; Amin, N.A.S.; Asmadi, M. Optimization of levulinic acid from lignocellulosic biomass using a new hybrid catalyst. *Bioresour. Technol.* **2012**, *116*, 58–65.

29. Qi, L.; Mui, Y.F.; Lo, S.W.; Lui, M.Y.; Akien, G.R.; Horváth, I.T. Catalytic Conversion of Fructose, Glucose, and Sucrose to 5-(Hydroxymethyl)furfural and Levulinic and Formic Acids in γ-Valerolactone as a Green Solvent. *ACS Catal.* **2014**, *4*, 1470–1477.

30. Shen, Y.; Xu, Y.; Sun, J.; Wang, B.; Xu, F.; Sun, R. Efficient conversion of monosaccharides into 5-hydroxymethylfurfural and levulinic acid in $InCl_3$-H_2O medium. *Catal. Commun.* **2014**, *50*, 17–20.